Portfolio optimization with digitized counterdiabatic quantum algorithms

N. N. Hegade [1,*] P. Chandarana [2,3,*] K. Paul [1] Xi Chen [2,3,†] F. Albarrán-Arriagada,[4,5,‡] and E. Solano [1,6,7,§]

[1]*International Center of Quantum Artificial Intelligence for Science and Technology (QuArtist) and*
Physics Department, Shanghai University, 200444 Shanghai, China
[2]*Department of Physical Chemistry, University of the Basque Country UPV/EHU, Apartado 644, 48080 Bilbao, Spain*
[3]*EHU Quantum Center, University of the Basque Country UPV/EHU, Barrio Sarriena, s/n, 48940 Leioa, Spain*
[4]*Departamento de Física, Universidad de Santiago de Chile (USACH), Avenida Víctor Jara 3493, 9170124 Santiago, Chile*
[5]*Center for the Development of Nanoscience and Nanotechnology 9170124, Estación Central, Santiago, Chile*
[6]*IKERBASQUE, Basque Foundation for Science, Plaza Euskadi 5, 48009 Bilbao, Spain*
[7]*Kipu Quantum, Kurwenalstrasse 1, 80804 Munich, Germany*

We consider digitized-counterdiabatic quantum computing as an advanced paradigm to approach quantum advantage for industrial applications in the NISQ era. We apply this concept to investigate a discrete mean-variance portfolio optimization problem, showing its usefulness in a key finance application. Our analysis shows a drastic improvement in the success probabilities of the resulting digital quantum algorithm when approximate counterdiabatic techniques are introduced. Along these lines, we discuss the enhanced performance of our methods over variational quantum algorithms like QAOA and DC-QAOA.

I. INTRODUCTION

Optimization problems have been of significant interest due to their fundamental applications in many fields such as logistics, medicine, and finance, among others. Nevertheless, due to their computational complexity, they cannot be solved efficiently using classical computers for industrial purposes. It is believed that a quantum computer might surpass the capabilities of a classical one. Due to the experimental developments during the last years, it might become useful for commercial purposes [1,2]. This potential breakthrough has boosted proposals of several algorithms in different areas, such as differential equations, linear algebra, and optimization problems [3], which have been implemented in small quantum computers as proof of principle. However, the applicability of these algorithms in the current noisy intermediate-scale quantum (NISQ) devices [4] is still under investigation. This is because of the difficulty to implement scalable error correction protocols with the current and near-future devices, a bottle neck for fault-tolerant quantum computing.

In recent years, the use of adiabatic quantum optimization (AQO) algorithms to solve optimization problems has received interest due to its experimentally feasible implementation [5–9]. These algorithms solve optimization problems by codifying them in the ground state of a Hamiltonian and accessing it via adiabatic evolution from another Hamiltonian, whose ground state is trivial to prepare. Current technology allows the implementation of incoherent adiabatic quantum computers or quantum annealers with thousands of qubits. Nevertheless, due to the considerable time involved in an adiabatic evolution, such devices have various limitations like noise and limited qubit connectivity. To overcome these difficulties, the use of digitized adiabatic quantum computing (DAdQC) [10] methods has been developed and implemented. These techniques are similar to AQO, but they digitized the evolution to implement the corresponding algorithms in a gate-based quantum computer. The convenience of digitization is that any arbitrary interactions can be included in the target Hamiltonian, providing more flexibility in choosing the optimization problem. However, it requires a large number of gates, which reduces the fidelity of the algorithms and makes them still impractical to approach quantum advantage in NISQ devices without error correction.

Other types of algorithms to solve optimization problems are the hybrid quantum-classical gate-based algorithms, like quantum approximate optimization algorithm (QAOA) [11]. In QAOA, a sequence of two evolutions is applied iteratively to an initial state. The evolution times are considered as free parameters to be optimized to minimize the cost function that encodes the solution to the problem. These evolutions are governed by a mixing Hamiltonian. Typically, a Pauli-X operation is applied to all the qubits and a problem Hamiltonian that codifies the cost function. Finally, the elapsed time of each evolution is optimized by a classical algorithm. Although QAOA is simple, it presents some major problems like the

---

*Co-first authors.

†chenxi1979cn@gmail.com

‡pancho.albarran@gmail.com

§enr.solano@gmail.com

number of algorithmic layers required to optimize the cost function. This issue, in general, is hard to solve for many-body Hamiltonians, limiting the possible scalability in current NISQ devices. Additionally, classical optimization does not guarantee the reach of the global minimum, as it can get stuck into local minima, or barren plateaus may appear [12–14].

To overcome these limitations, shortcuts to adiabaticity (STA) methods were proposed. These are known to improve the adiabatic processes by circumventing the need of slow driving [15]. STA includes methods like fast-forward [16,17], invariant based inverse engineering [18,19], and counterdiabatic (CD) driving [20–24]. Among these, CD driving, i.e., the addition of an extra term that suppresses the non-adiabatic transitions, has already shown improvements in adiabatic quantum computing [25,26] and quantum annealing [27–29].

Recently, Hegade *et al.* showed the advantage of CD driving in DAdQC methods [25], which have shown interesting improvements in many-body ground state preparations and adiabatic quantum factorization problems [26]. It was also studied that the inclusion of these approximate counterdiabatic terms could enhance the performance of QAOA while solving combinatorial optimization problems and state preparation of many-body ground states [30–32]. This article considers the advantages of digitized-counterdiabatic quantum computing (DCQC) and digitized-counterdiabatic quantum approximate optimization algorithms (DC-QAOA) in financial applications. In particular, we investigate the Markowitz portfolio optimization problem [33], a common problem used intensively by financial asset managers and is. This problem deals with how to optimize the weights of the assets in a portfolio to give out returns based on the requirements of the asset manager, as is the case of maximum return and minimum risk. We select a large number of data instances and solve the problem using the DAdQC combined with CD-driving protocols. By considering variational minimization techniques, we obtain the approximate CD terms, getting a drastic enhancement in the success probability for most of selected instances. We also show that inclusion of these CD terms in hybrid quantum-classical algorithms like QAOA, namely DC-QAOA, results in improvement of success probabilities. This article demonstrates the relevance of CD driving, its limitations, and applicability for finance industry problems in the NISQ era.

The manuscript is arranged as follows. In the following section Sec. II, we present the theory of the Markowitz portfolio optimization problem and how to encode it as a quadratic unconstrained binary optimization problem, which can later map to finding the ground state of an Ising Hamiltonian. In Sec. III, we formulate the digitized-counterdiabatic techniques to enhance the performance of adiabatic quantum algorithms for obtaining the approximate ground states in a finite time. We consider local CD driving and approximate CD terms and show their performance for solving different instances of the portfolio optimization problem with ideal simulations and noisy simulations with Quantinuum's trapped-ion quantum emulator. Section IV considers the hybrid quantum-classical algorithms like QAOA and DC-QAOA to tackle the same problem and compare their performance. Finally, in Sec. V, we discuss our results and conclude.

II. PRELIMINARIES

Suppose an asset manager is willing to invest a budget b in a given portfolio with n number of assets. Markowitz portfolio optimization [33] answers the question: How to distribute the given budget b into n assets such that the asset manager would receive maximum returns at minimum risk. For example, the asset manager could invest evenly in all the assets, but that may not be the best choice. Given the expected returns of each asset x_i and the risk associated with the assets, applying Markowitz portfolio optimization, we can predict the distribution of the budget b to get the maximum returns out of the portfolio. Expected returns can be estimated from the preceding market return data, and the risk is assessed via a covariance matrix. As the name suggests, a covariance matrix shows the covariance of different stocks in the portfolio. Thus, these types of problems are classified as mean-variance portfolio optimization problems.

The portfolio optimization problem has two components, the cost function and the constraints. The cost function includes quantities such as the average returns, the variance of the portfolio, and others that need to be maximized or minimized based upon the need of the asset manager, while the constraints can include budget constraints or transition costs or market inflation. Based on the constraints, the portfolio optimization problems can be broadly divided into three types. The first type of optimization problem is the unconstrained portfolio optimization, where the constraints are added as the penalty terms in the cost function with the help of Lagrange multipliers. The second type is when the constraints can be represented as inequalities, and the third type is when the constraints are the integer constraints, the so-called mixed-integer problem. Examples and computational complexities of all these problems are discussed in Ref. [34]. Different types of these portfolio optimization problems have been studied recently using quantum computing [35–39], and quantum annealing methods [40–42].

As far as the variables are concerned, portfolio optimization can be solved as a continuous-variable and discrete-variable problem. Discrete mean-variance optimization proves to be a beneficial method to optimize the given portfolio in cases where the assets are traded in lots, which are integer multiples of a base size of assets traded. Thus, the asset manager will only be interested in the number of lots which makes the problem discrete. In consequence, using the digitized-counterdiabatic quantum computing paradigm, we will investigate here an unconstrained single-period discrete mean-variance portfolio optimization which is in general an NP-complete optimization problem. This complexity is discussed in detail in Ref. [43] where authors discuss that the inclusion of real features like transaction costs and budget requirements makes this a complex mathematical problem.

Our task is to distribute b budget into n assets with mean returns m_i and the covariance matrix ρ_{ij} to maximize returns at a minimum variance. The problem can be formulated as,

$$\max_x \sum_{i=1}^{n} \theta_1 m_i x_i - \theta_2 \rho_{ij} x_i x_j - \theta_3 (G_f b x_i - b)^2, \quad (1)$$

where x_i are the assets represented by integers. The first term of Eq. (1) indicates the expected returns, where m_i are the daily return data, and the second term shows the variance of the portfolio, where ρ_{ij} show the variance of jth asset with i. The market data (m_i and ρ_{ij}) is easily available and can be generated in various ways [44,45]. The third term shows the constraint applied to the budget. Most of the times, asset managers have a certain budget to follow, so this term penalizes the solutions that do not satisfy the budget criteria. The term G_f in Eq. (1) shows the granularity function which is given by $G_f = 1/2^{(g-1)}$, where g is the number of slices of the budget. This implies that the fraction of the budget that can be chosen is $G_f b x_i$. To explain this, assume that we set $g = 2$, so the budget is cut into two slices giving $G_f = 1/2$. Therefore, we have $b/2$ weight of the budget that can be invested in required assets. In other words, granularity function decides how small a fraction of b you can invest in a particular stock. Thus, with increasing the value of slice g, we get the freedom to invest smaller fractions of the budget which will give us more precision while deciding the optimal results. θ_1, θ_2, and θ_3 are the Lagrange multipliers and their role is to adjust weights of different terms to adjust constraints according to the manager's requirements. For instance, if the manager is less concerned about the risk and more interested about the returns, we can set θ_1 higher than θ_2 such that the expected return term is given more weight.

Once these terms are determined, we can convert Eq. (1) into an Ising Hamiltonian. To do so, we start with transforming Eq. (1) into a quadratic unconstrained binary optimization problem (QUBO) by encoding assets x_i integers into an g bit binary number. Apart from binary encoding, various ways of encoding like unary, sequential, and partition have been proposed [41]. Hence, x_i's are given by

$$x_i = \sum_{k=1}^{g} 2^{k-1} z_{u(i,k)}, \tag{2}$$

where $u(i, k) = (i - 1)g + k$ and $z \in \{0, 1\}$. This problem can be transformed into a QUBO problem by substituting x_i's from Eq. (2) into Eq. (1). After making some rearrangements and transformation of $z_i = \frac{1}{2}(1 + \sigma_i^z)$, we get an Ising Hamiltonian given by

$$H_p = \sum_i h_i \sigma_i^z + \sum_{i,j} J_{ij} \sigma_i^z \sigma_j^z + \beta, \tag{3}$$

where J_{ij} shows the interaction coefficient between the spins i and j, while h_i shows the coefficient associated with the local field along the z axis. Explicit forms of these coefficients are given by

$$J_{ij} = \frac{1}{4}\left(\theta_2 b^2 G_f^2 + \theta_3 \rho_{i,j}\right), \tag{4}$$

$$h_i = \frac{(-\theta_1 m_i - 2\theta_2 b^2 G_f)}{2} + \sum_j J_{i,j}, \tag{5}$$

with a constant β that can be ignored. In this manner, we have transformed Eq. (1) into an Ising Hamiltonian such that its ground state encodes the solution to the optimization problem. In the following sections we show application of

digitized-counterdiabatic quantum computing methods to find this ground state.

III. DIGITIZED-COUNTERDIABATIC QUANTUM COMPUTING

To find the ground state of the Hamiltonian in Eq. (3), we follow the adiabatic theorem by starting with an initial Hamiltonian whose ground state can be easily prepared, and slowly turn on the problem Hamiltonian. The corresponding total Hamiltonian is given by

$$H_{ad}(\lambda) = (1 - \lambda)H_i + \lambda H_p, \tag{6}$$

where λ is a time dependent scheduling function. We choose the initial Hamiltonian as $H_i = -\sum_i^N h^x \sigma_i^x$, whose ground state $|\psi(0)\rangle = 2^{-N/2}(|0\rangle + |1\rangle)^{\otimes N}$ can be easily prepared. If the evolution is slow enough, the adiabatic theorem guarantees that the final state will have a large overlap with the ground state of the problem Hamiltonian. In principle, to obtain the ground state with a higher success probability, one has to consider the total evolution time T much larger than the minimum energy gap $\Delta_{\min}$ between the ground state and the first excited state. However, in practice, one cannot rely on the adiabatic evolution due to limited coherence time and device noise. One has to consider a short time evolution that will lead to nonadiabatic transitions between the eigenstates. In order to suppress these transitions, a technique called shortcuts to adiabaticity was developed [46,47]. The idea is to introduce an additional term called counterdiabatic-driving term (CD term) so that the excitations due to the finite time evolution will be compensated, and the resulting evolution will be quasiadiabatic. The modified Hamiltonian by adding the CD term takes the form

$$H(t) = H_{ad} + \dot{\lambda} A_{\lambda}, \tag{7}$$

where A_{λ} is called adiabatic gauge potential [48], which satisfies the condition $[i\partial_{\lambda}H_{ad} - [A_{\lambda}, H_{ad}], H_{ad}] = 0$. In principle, one can evolve the system very fast without any excitation by including the CD term. However, obtaining the exact gauge potential for a many-body system is a difficult task. Also, the operator form of the CD term for a many-body system with N interacting spins generally contains nonlocal N-body interaction terms, which makes it experimentally challenging to realize. To overcome this challenge a variational method was proposed to obtain an approximate CD term [48]. And, many recent works show the advantage of using variationally calculated local CD terms for different applications [22,49,50]. The main advantage of this method is that the approximate local CD terms can be easily implemented in laboratory and its calculation does not require any knowledge of the instantaneous eigenstates. This feature makes it suitable for adiabatic quantum computation.

For the Hamiltonian (3), we choose the local CD term of the form $\tilde{A}_{\lambda} = \sum_i^N \alpha_i(t)\sigma_i^y$. Here, the CD coefficient $\alpha_i(t)$ is obtained by minimizing the action $S = \text{Tr}[G_{\lambda}^2]$, where $G_{\lambda} = \partial_{\lambda}H_{ad} + i[\tilde{A}_{\lambda}, H_{ad}]$,

$$\alpha_i(t) = -\frac{h^x h_i^z}{2\left(h^{x2}[\lambda - 1]^2 + \lambda^2\left[h_i^{z2} + \sum_{i \neq j} J_{ij}^2\right]\right)}. \tag{8}$$
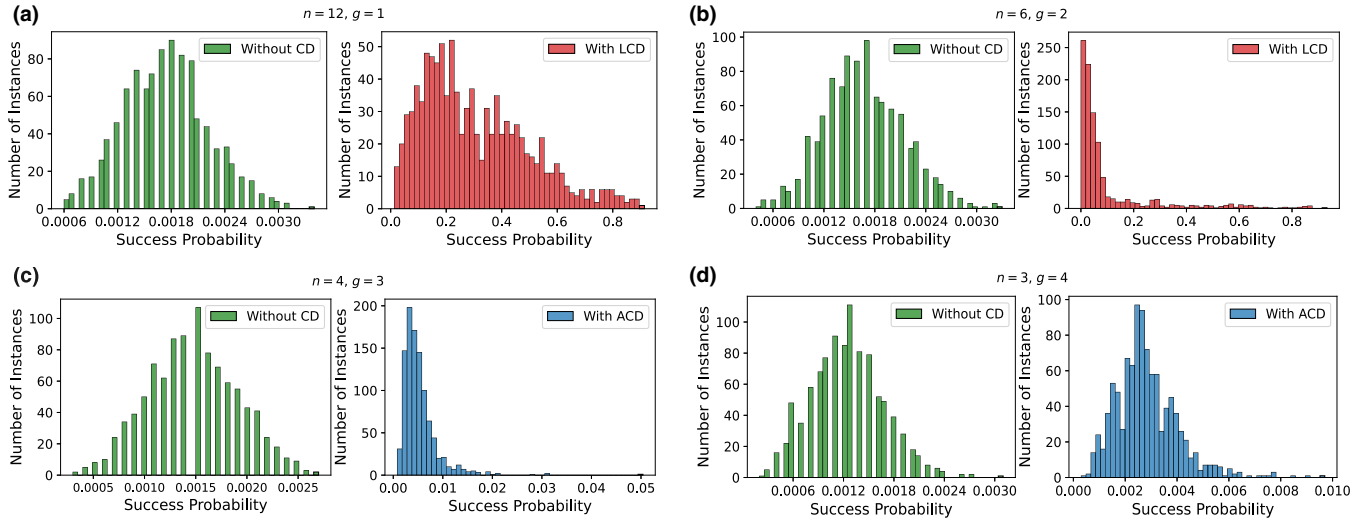
FIG. 1. Histogram depicts the ground state success probability for 1000 randomly chosen instances of the portfolio optimization problem with and without CD driving. We considered 12 qubit systems with different numbers of assets (n) and partitions (g). When the number of partitions is smaller, the LCD in Eq. (8) gives a better enhancement. Whereas, when g is larger, ACD from Eq. (12) shows greater improvement. The simulation parameters are: total evolution time $T = 1$, and the step size $\Delta t = 0.05$.

The CD term should vanish at the beginning and end of the protocol, for that we consider the scheduling function as $\lambda(t) = \sin^2[\frac{\pi}{2} \sin^2(\frac{\pi t}{2T})]$, also $\dot{\lambda}$, and $\ddot{\lambda}$ vanishes at $t = 0$ and $t = T$. The time evolution including the CD term is given by

$$|\psi(T)\rangle = \mathcal{T}e^{-i \int_0^T H(t)dt} |\psi(0)\rangle = U(0, T) |\psi(0)\rangle . \quad (9)$$

For the gate-model implementation of the evolution, we write the total Hamiltonian as the sum of 2-local terms, i.e., $H(t) = \sum_j c_j(t)H_j(t)$. We discretize the total time into M parts with step size $\Delta t = T/M$. Using Trotter-Suzuki formula, we approximate the time evolution operator as

$$U_{\text{dig}}(0, T) = \prod_{k=1}^{M} \prod_{j} \exp\{-i\Delta t c_j(k\Delta t)H_j\}. \quad (10)$$

In this work, we only considered first-order trotterization, which leads to an error of the order $\mathcal{O}(\Delta t^2)$. Using single-qubit and two-qubit gates, each matrix exponential term in Eq. (10) can be easily implemented. Since the Hamiltonian involves all-to-all connection between the qubits, extra swap gates might be needed on a device with only nearest neighbor interactions. We consider a wide range of portfolios where the data (m_i and ρ_{ij}) is randomly generated such that it mimics the real world trends. $\theta_1 = 0.3$, $\theta_2 = 0.5$, and $\theta_3 = 0.2$ are selected so that the budget constraint is given greater importance. We run 1000 different instances and system sizes up to $N = 14$ qubits with a different number of stocks n and slicing g.

Since current NISQ devices can only implement circuits of limited depth, we consider a short-time evolution and compare the final success probability with and without including the CD term. In Fig. 1, the ground state success probability for 1000 randomly chosen instances of the portfolio optimization problem is depicted for a system size $N = 12$. In Fig. 1(a), the number of assets and the slices are chosen as $n = 12$, $g = 1$, respectively. And, in Fig. 1(b), $n = 6$, $g = 2$. We fix the total evolution time $T = 1$, and step size $\Delta t = 0.05$ with total 20

Trotter steps. In both cases, the local CD (LCD) term $H_{\text{LCD}} = \dot{\lambda} \sum_i^N \alpha_i(t)\sigma_i^y$ is considered.

We observe that when the number of slices is less, the LCD terms drastically improves the success probability for most of the instances. However, as g becomes larger, the performance of LCD terms will be decreased. Previously, it was shown that the density of states close to the ground state would also become larger with the increasing number of slices, leading to an increase in the probability of transition to the higher excited states [40]. In order to suppress these transitions, we considered higher-order CD terms obtained by the nested commutator (NC) ansatz [51],

$$A_\lambda^{(l)} = i \sum_{k=1}^{l} \alpha_k(t) \underbrace{[H_{ad}, [H_{ad}, ...[H_{ad}}_{2k-1}, \partial_\lambda H_{ad}]]]. \quad (11)$$

Here, l corresponds to the expansion order, and when $l \to \infty$ we will get the exact gauge potential. By considering the first-order expansion ($l = 1$), we obtain the approximate CD (ACD) term for the problem Hamiltonian in Eq. (3) as

$$H_{\text{ACD}} = 2\dot{\lambda}h^x\alpha_1(t) \left[\sum_i^N h_i^z \sigma_i^y + \sum_{i,j} J_{ij}\left(\sigma_i^y \sigma_j^z + \sigma_i^z \sigma_j^y\right) \right], \quad (12)$$

where $\alpha_1(t)$ is obtained as before by minimization of the action $S = \text{Tr}[G_\lambda^2]$. The general expression for $\alpha_1(t)$ for an Ising spin-glass Hamiltonian is given in [52]. In Figs. 1(c) and 1(d), we considered $g = 3$ and $g = 4$, respectively, and compare the probability of success for different instances by including ACD and without including the CD term. The CD solutions depend upon the choice of instances which can be either easy or hard depending on the value of the slicing parameter g. As follows from Eqs. (4) and (5), the local field h_i is significantly large compared to the interaction term J_{ij} for lower values of g that translates into a weakly coupled Ising system. Consequently, for $h_i \gg J_{ij}$, the success probability
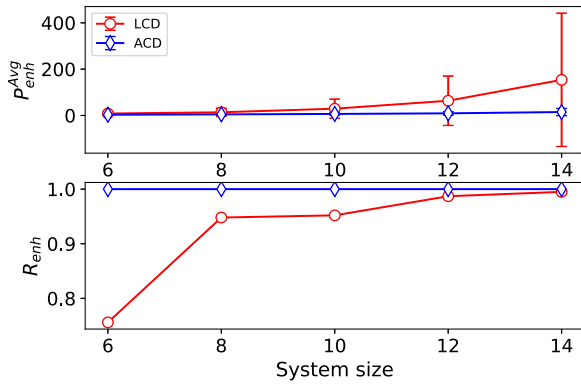
FIG. 2. The upper plot depicts the average success probability enhancement [Eq. (14)], and the lower plot represents the enhancement ratio [Eq. (13)] for various system sizes with LCD and ACD. The error bars represent the standard deviation. Due to the huge variations in the success probability enhancement for different instances using LCD, the error bars have larger values.

FIG. 3. Output probability distribution of an instance with $n = 3$ and $g = 2$. We considered $T = 0.3$ and $\delta t = 0.1$. The green bar corresponds to the results obtained from Quantinuum's H1 emulator, which mimics the noise model of the hardware Model H1. The red and blue bars are for the ideal simulation results with and without including the CD terms, respectively. The ground-state bitstring is also shown.

can be improved drastically using the Local CD driving due to relatively larger energy gaps which is in accordance with Figs. 1(a) and 1(b) [25]. Such instances are referred to as the easy ones. On the other hand, the hard instances occur when g is large, we obtain a strongly coupled Ising Hamiltonian where $h_i \approx J_{ij}$. In such cases, we need to take aid of the approximate CD driving to show the enhancement in the success probability [see Figs. 1(c) and 1(d)]. Nonetheless, in both the cases, we can obtain an enhancement at least up to an order of magnitude.

To show the enhancement that results from applying the CD term, we define a metric called enhancement ratio,

$$R_{\text{enh}} = \frac{I}{I^0}, \tag{13}$$

where I^0 is the total number of instances considered, and I denotes the number of instances with enhanced success probability by including the CD term. The enhancement that results from applying the CD term is quantified by the success probability enhancement,

$$P_{\text{enh}} = \frac{P}{P^0}. \tag{14}$$

Here, P is the ground state success probability by including the CD term, and P^0 is the success probability obtained by naive evolution without the CD term. Figure 2 depicts the average success probability enhancement and enhancement ratio for various system sizes by including the CD driving. We observed that for ACD, the enhancement ratio is 1, indicating that it is always advantageous to include the approximate CD terms obtained from the first order NC ansatz with fixed $g = 2$. The simulation result indicates that the enhancement with the CD term will increase with the system size. In Fig. 4, the ground state success probability as a function of total evolution time T is shown. The result shows that a huge enhancement can be obtained for both LCD and ACD. For Fig. 4, we selected 40 random instances, and each colored line depicts one of the instances considered. It can be observed that two particular instances achieve better success probability than the rest while using LCD. This is due to the fact that those
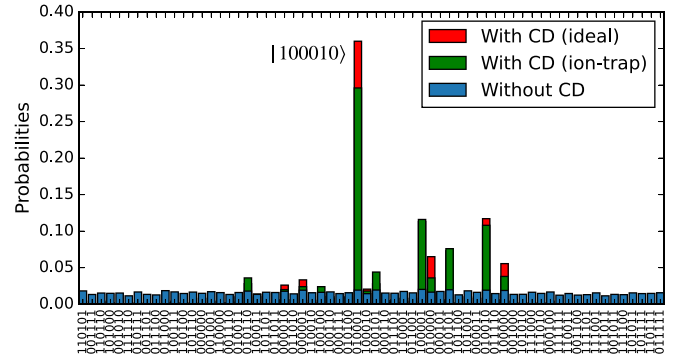
particular easy instances have a significantly larger energy gap compared to other instances. This can be verified from Fig. 4(a) where, even in the adiabatic case, those two instances give better success probability referring to the existence of a larger gap, which makes the suppression of nonadiabatic contributions easier with LCD.

To make our arguments even more concrete, we also implemented a $N = 6$ qubit system with $n = 3$, $g = 2$ on an emulator that closely mimics the noise model of the hardware *Quantinuum System Model H1* [53], which is an all-to-all connected trapped-ion quantum computing system with 20 qubits. Trapped-ion systems are a good choice for this problem because of their all-to-all connectivity, making it easier to implement the interactions without using any additional SWAP gates. In our implementation, we initialize all the qubits in $|+\rangle$ state, which corresponds to the ground state of the initial Hamiltonian and then apply the digitized time evolution with the help of the native gates provided by the device. As the two-qubit $ZZ(\theta)$ gate is native to this hardware, we can efficiently implement the matrix exponential terms in Eq. (10) without relying on the standard decomposition with CNOTs. And finally, we measure the final state on a computational basis. We have selected a total time evolution for the noisy simulation as $T = 0.3$, with step size $\delta t = 0.1$, which gives three trotter steps. The number of shots is set to $N_{\text{shots}} = 500$ and the ground-state of the instance we investigate is $GS = |100010\rangle$. Since the time scale we chose is small, the CD terms are dominant for this fast evolution. While implementing on the hardware, we could discard the term H_{ad} to reduce the gate counts without affecting the success probability. In Fig. 3, we have plotted the probability distribution obtained at the end of the evolution without CD term and with ACD. Even with just three trotter steps, the evolution with ACD gives the ground state with very high success probability compared to the without CD case. We remark that this performance will be similar when the real device is used. Evidently CD driving does perform well even in the presence of noise, and we can still get a drastic enhancement over the usual digitized
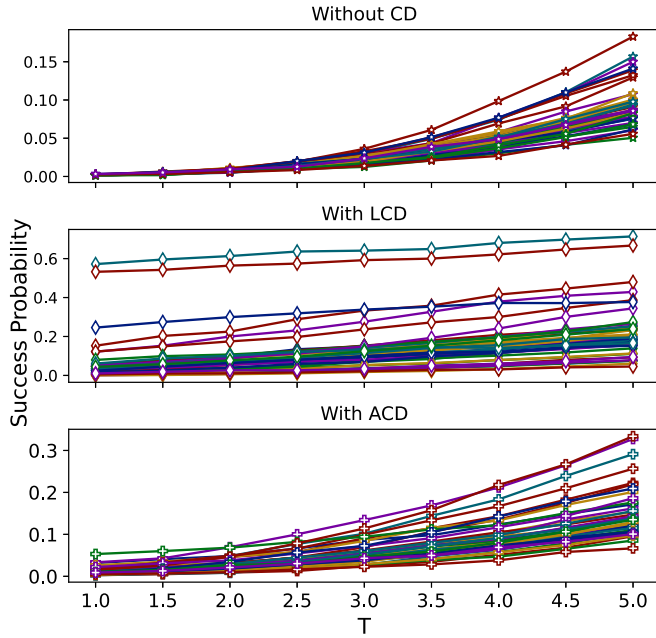
FIG. 4. Success probability as a function of total evolution time T for randomly chosen 40 instances is depicted. Here we considered $n = 6$ assets and $g = 2$ partitions resulting in system size $N = 12$. A substantial improvement in success probability is obtained for most of the instances by including the local CD term H_{LCD}, and the approximate CD term H_{ACD}. Here we considered the Trotter step size as $\Delta t = 0.1$. Different colored lines show each of the 40 instances.

FIG. 5. Average success probability (P_s) as a function of number of layers for a $N = 6$ system with $n = 3$, $g = 2$. Results show mean success probability obtained after considering 10 instances and 20 random initializations in each instance. Error bars represent variance of the distribution. Stochastic gradient descent based optimizer called adagrad optimizer with step size $= 0.1$ was used as the classical optimizer for all instances.

adiabatic evolution making our algorithm suitable for NISQ devices.

IV. DIGITIZED-COUNTERDIABATIC QUANTUM APPROXIMATE OPTIMIZATION ALGORITHM (DC-QAOA)

Hybrid quantum-classical optimization algorithms like QAOA [11] have been of interest due to their applicability in the noisy intermediate-scale quantum (NISQ) devices. These algorithms fall under the class of variational quantum algorithms, where classical optimization routines are employed to find suitable parameters (γ, β) that optimize a cost function $C(\gamma, \beta)$. In our case, we have set $C(\gamma, \beta) = \langle \psi_f(\gamma, \beta) | H_p | \psi_f(\gamma, \beta) \rangle$ such that $C(\gamma, \beta)$ shows the expectation value of the problem Hamiltonian H_p and $|\psi_f(\gamma, \beta)\rangle$ is given by,

$$|\psi_f(\gamma, \beta)\rangle = U(\gamma, \beta) |\psi_i\rangle, \tag{15}$$

where $|\psi_i\rangle = |+\rangle^{\otimes N}$ is the initial state corresponding to the mixer Hamiltonian and,

$$U(\gamma, \beta) = U_m(\beta_p) U_c(\gamma_p) U_m(\beta_{p-1}) U_c(\gamma_{p-1})$$
$$\dots U_m(\beta_1) U_c(\gamma_1). \tag{16}$$

Here, $U_b(\beta)$ and $U_c(\gamma)$ are two unitaries corresponding to the mixer and the problem Hamiltonian, respectively, applied iteratively for p layers. At $p \to \infty$, QAOA is expected to converge to the ground state of any problem Hamiltonian because it mimics the adiabatic evolution. However, experimentally realising large p circuits is difficult due to the noise,
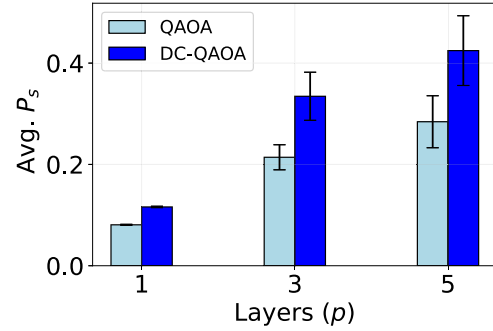
hence, significant research has been done recently to improve the performance of low p QAOA circuits. Over the years, many modifications have been reported in the standard QAOA [30–32,54–56] to serve this purpose. Among them, the addition of terms using counterdiabatic (CD) protocols has shown significant improvements, specially in finding the ground state of many-body Hamiltonians [30–32]. One of the algorithms following the same principle is the digitized-counterdiabatic quantum approximate optimization algorithm (DC-QAOA) [31]. In DC-QAOA, CD protocol is utilized to introduce an additional CD unitary $U_D(\alpha)$. The form of CD unitary is chosen from the operator pool $A_\lambda^{(l)}$ obtained using the nested commutator (NC) method as mentioned in Sec. III. Therefore, three unitaries $U_b(\beta)$, $U_c(\gamma)$, and $U_D(\alpha)$ are applied iteratively while performing DC-QAOA. In this section, we perform QAOA and DC-QAOA for 10 instances of portfolios with system size $N = 6$ qubits ($n = 3$, $g = 2$) with $\theta_1 = 0.3$, $\theta_2 = 0.5$, and $\theta_3 = 0.2$ to compare the obtained success probabilities (P_s) and demonstrate the advantage of CD-induced variational quantum algorithms for portfolio optimization. In QAOA, p layers of $U_b(\beta) = e^{-i\beta \sum_i \sigma_i^x}$ and $U_p(\gamma) = e^{-i\gamma H_p}$, where H_p is given by Eq. (3), are applied to the initial state $|\psi_i\rangle$. In DC-QAOA, $U_D(\alpha) = e^{-i\alpha \sum_i h_i \sigma_i^y}$ is added, where σ^y is a local first-order term chosen from an operator pool $A_\lambda^{(2)} = \{\sigma^y, \sigma^z \sigma^y, \sigma^y \sigma^z, \sigma^x \sigma^y, \sigma^y \sigma^x\}$ which is obtained from Eq. (11). Parameters (γ, β, α) are updated using a stochastic gradient descent (SGD) based classical optimizer called Adagrad optimizer [57] with step size $= 0.1$.

Figure 5 shows the mean success probabilities (P_s) as a function of number of layers (p) for $N = 6$ system with $n = 3$, $g = 2$. Results show mean of the 10 different instances where each instance is best output chosen from 20 runs of different random initial parameters for each layer. We observe that by using DC-QAOA, improvement in the P_s value is achieved for all the instances. The higher error bars shows that even for the same system size and values of n and g, the performance of DC-QAOA and QAOA depends upon the the energy landscape and the choice of the CD operator. This improvement by using DC-QAOA can be attributed to the fact that the introduction of a free parameter makes the Hilbert

space more accessible to the optimizer so it increases the expressibility of the circuit ansatz. The high variances can also be attributed to the fact that the performance of these algorithms depend upon the initial parameters and the classical optimizer chosen. In particular, classical optimizers and their step sizes play a significant role in improving the performance of the algorithm. Nevertheless, a considerable improvement can always be achieved using DC-QAOA over conventional QAOA algorithm. Moreover, here we have used local CD operators only, but in the typical hard instances, higher-order CD terms might give more improvement. However, inclusion of these higher-order CD terms might also increase the effective circuit depth to a larger extent which can induce errors, reducing the advantages of DC-QAOA.

V. CONCLUSION

We studied the financial portfolio optimization problem using recently proposed digitized-counterdiabatic quantum algorithms. We computed the approximate CD terms that can be easily implemented on any current gate-based quantum computer. We compared the ground state success probability for the evolution with and without including the CD terms, by fixing the total evolution time or the number of Trotter steps. We considered many instances of the portfolio optimization problem with randomly generated data. The results indicate that, for most cases, the inclusion of the local CD term and approximate CD term substantially improves the success probability. We also verified this behavior by considering the noisy emulator of a trapped-ion system with all-to-all connected qubits. As expected, we get an advantage over the state-of-the-art methods when noise is present in the system. Also, we consider the hybrid classical-quantum algorithms for tackling hard instances of the portfolio optimization problem. In particular, we considered QAOA and DC-QAOA methods and showed that CD-assisted QAOA gives better performance than the naive approach. However, for random

initialization, finding optimal parameters for QAOA and DC-QAOA is a challenging task due to the highly nonconvex nature of the cost landscape. Moreover, a hybrid quantum-classical algorithm can face challenges such as local-minima, noise-induced barren plateaus, etc.

In conclusion, adding the local and approximate CD terms provides a drastic enhancement for solving the portfolio optimization problem by finite-time adiabatic evolution and also for hybrid classical-quantum algorithms. The present study considers only 2-local CD terms. Extending this to higher-order terms is expected to give further enhancement. This article presents an interesting approach to address the portfolio optimization problem using the digitized-counterdiabatic method. However, one should note that the counterdiabatic method is ubiquitous in nature and can be applied to a wide range of combinatorial optimization problems in the quantum computing paradigm. As an outlook, to consider the development of a digital-analog quantum computing encoding, on top of the digitized-counterdiabatic quantum algorithm for solving the same problem, may approach us to quantum advantage for industrial use cases in the NISQ era.

[1] M. Mohseni, P. Read, H. Neven, S. Boixo, V. Denchev, R. Bab-bush, A. Fowler, V. Smelyanskiy, and J. Martinis, Commercialize quantum technologies in five years, Nature (London) **543**, 171 (2017).

[2] F. Bova, A. Goldfarb, and R. G. Melko, Commercial applications of quantum computing, EPJ Quantum Technol. **8**, 2 (2021).

[3] A. Montanaro, Quantum algorithms: An overview, npj Quantum Inf. **2**, 1 (2016).

[4] J. Preskill, Quantum computing in the NISQ era and beyond, Quantum **2**, 79 (2018).

[5] E. Farhi, J. Goldstone, S. Gutmann, J. Lapan, A. Lundgren, and D. Preda, A Quantum adiabatic evolution algorithm applied to random instances of an NP-Complete problem, Science **292**, 472 (2001).

[6] A. P. Young, S. Knysh, and V. N. Smelyanskiy, First-Order Phase Transition in the Quantum Adiabatic Algorithm, Phys. Rev. Lett. **104**, 020502 (2010).

[7] X. Peng, Z. Liao, N. Xu, G. Qin, X. Zhou, D. Suter, and J. Du, Quantum Adiabatic Algorithm for Factorization and Its Experimental Implementation, Phys. Rev. Lett. **101**, 220405 (2008).

[8] M. Steffen, W. van Dam, T. Hogg, G. Breyta, and I. Chuang, Experimental Implementation of an Adiabatic Quantum Optimization Algorithm, Phys. Rev. Lett. **90**, 067903 (2003).

[9] V. Bapst, L. Foini, F. Krzakala, G. Semerjian, and F. Zamponi, The quantum adiabatic algorithm applied to random optimization problems: The quantum spin glass perspective, Phys. Rep. **523**, 127 (2013).

[10] R. Barends, A. Shabani, L. Lamata, J. Kelly, A. Mezzacapo, U. Las Heras, R. Babbush, A. G. Fowler, B. Campbell, Y. Chen, Z. Chen, B. Chiaro, A. Dunsworth, E. Jeffrey, E. Lucero, A. Megrant, J. Y. Mutus, M. Neeley, C. Neill, P. J. J. O'Malley, C. Quintana *et al.*, Digitized adiabatic quantum computing with a superconducting circuit, Nature (London) **534**, 222 (2016).

[11] E. Farhi, J. Goldstone, and S. Gutmann, A Quantum approximate optimization algorithm, arXiv:1411.4028.

[12] E. Grant, L. Wossnig, M. Ostaszewski, and M. Benedetti, An initialization strategy for addressing barren plateaus in parametrized quantum circuits, Quantum **3**, 214 (2019).

[13] J. R. McClean, S. Boixo, V. N. Smelyanskiy, R. Babbush, and H. Neven, Barren plateaus in quantum neural network training landscapes, Nat. Commun. **9**, 4812 (2018).

[14] M. Cerezo, A. Sone, T. Volkoff, L. Cincio, and P. J. Coles, Cost function dependent barren plateaus in shallow parametrized quantum circuits, Nat. Commun. **12**, 1791 (2021).

[15] K. Takahashi, Hamiltonian engineering for adiabatic quantum computation: Lessons from shortcuts to adiabaticity, J. Phys. Soc. Jpn. **88**, 061002 (2019).

[16] S. Masuda and K. Nakamura, Fast-forward of adiabatic dynamics in quantum mechanics, Proc. R. Soc. A **466**, 1135 (2010).

[17] S. Masuda and K. Nakamura, Fast-forward problem in quantum mechanics, Phys. Rev. A **78**, 062108 (2008).

[18] X. Chen, A. Ruschhaupt, S. Schmidt, A. del Campo, D. Guéry-Odelin, and J. G. Muga, Fast Optimal Frictionless Atom Cooling in Harmonic Traps: Shortcut to Adiabaticity, Phys. Rev. Lett. **104**, 063002 (2010).

[19] X. Chen, E. Torrontegui, and J. G. Muga, Lewis-Riesenfeld invariants and transitionless quantum driving, Phys. Rev. A **83**, 062116 (2011).

[20] M. Demirplak and S. A. Rice, Assisted adiabatic passage revisited, J. Phys. Chem. B **109**, 6838 (2005).

[21] M. Demirplak and S. A. Rice, Adiabatic population transfer with control fields, J. Phys. Chem. A **107**, 9937 (2003).

[22] L. Prielinger, A. Hartmann, Y. Yamashiro, and K. Nishimura, Two-parameter counter-diabatic driving in quantum annealing, Phys. Rev. Res. **3**, 013227 (2021).

[23] A. del Campo, Shortcuts to Adiabaticity by Counterdiabatic Driving, Phys. Rev. Lett. **111**, 100502 (2013).

[24] A. B. Özgüler, R. Joynt, and M. G. Vavilov, Steering random spin systems to speed up the quantum adiabatic algorithm, Phys. Rev. A **98**, 062311 (2018).

[25] N. N. Hegade, K. Paul, Y. Ding, M. Sanz, F. Albarrán-Arriagada, E. Solano, and X. Chen, Shortcuts to Adiabaticity in Digitized Adiabatic Quantum Computing, Phys. Rev. Appl. **15**, 024038 (2021).

[26] N. N. Hegade, K. Paul, F. Albarrán-Arriagada, X. Chen, and E. Solano, Digitized adiabatic quantum factorization, Phys. Rev. A **104**, L050403 (2021).

[27] W. Vinci and D. A. Lidar, Non-stoquastic Hamiltonians in quantum annealing via geometric phases, npj Quantum Inf. **3**, 38 (2017).

[28] K. Takahashi, Shortcuts to adiabaticity for quantum annealing, Phys. Rev. A **95**, 012309 (2017).

[29] G. Passarelli, V. Cataudella, R. Fazio, and P. Lucignano, Counterdiabatic driving in the quantum annealing of the p-spin model: A variational approach, Phys. Rev. Res. **2**, 013283 (2020).

[30] J. Yao, L. Lin, and M. Bukov, Reinforcement Learning for Many-Body Ground-State Preparation Inspired by Counterdiabatic Driving, Phys. Rev. X **11**, 031070 (2021).

[31] P. Chandarana, N. N. Hegade, K. Paul, F. Albarrá n-Arriagada, E. Solano, A. del Campo, and X. Chen, Digitized-counterdiabatic quantum approximate optimization algorithm, Phys. Rev. Res. **4**, 013141 (2022).

[32] J. Wurtz and P. J. Love, Counterdiabaticity and the quantum approximate optimization algorithm, Quantum **6**, 635 (2022).

[33] H. Markowitz, Portfolio selection, J. Finance **7**, 77 (1952).

[34] A. Bouland, W. van Dam, H. Joorati, I. Kerenidis, and A. Prakash, Prospects and challenges of quantum finance, arXiv:2011.06492.

[35] M. Hodson, B. Ruck, H. Ong, D. Garvin, and S. Dulman, Portfolio rebalancing experiments using the Quantum Alternating Operator Ansatz, arXiv:1911.05296.

[36] M. Marzec, Portfolio optimization: Applications in quantum computing, Handbook of high-frequency trading and modeling in finance, 73 (2016), https://papers.ssrn.com/sol3/papers.cfm?abstract_id=2278729.

[37] P. Rebentrost and S. Lloyd, Quantum computational finance: quantum algorithm for portfolio optimization, arXiv:1811.03975.

[38] R. Orús, S. Mugel, and E. Lizaso, Quantum computing for finance: Overview and prospects, Rev. Phys. **4**, 100028 (2019).

[39] S. Mugel, C. Kuchkovsky, E. Sanchez, S. Fernandez-Lorenzo, J. Luis-Hita, E. Lizaso, and R. Orús, Dynamic portfolio optimization with real datasets using quantum processors and quantum-inspired tensor networks, Phys. Rev. Res. **4**, 013006 (2022).

[40] E. Grant, T. S. Humble, and B. Stump, Benchmarking Quantum Annealing Controls with Portfolio Optimization, Phys. Rev. Appl. **15**, 014012 (2021).

[41] G. Rosenberg, P. Haghnegahdar, P. Goddard, P. Carr, K. Wu, and M. L. de Prado, Solving the optimal trading trajectory problem using a quantum annealer, IEEE J. Sel. Top. Signal Process. **10**, 1053 (2016).

[42] D. Venturelli and A. Kondratyev, Reverse quantum annealing approach to portfolio optimization problems, Quantum Mach. Intell. **1**, 17 (2019).

[43] H. Kellerer, R. Mansini, and M. G. Speranza, Selecting portfolios with fixed costs and minimum transaction lots, Ann. Operations Res. **99**, 287 (2000).

[44] X. Huang, Meann "variance models for portfolio selection subject to experts" estimations, Expert Systems Applications **39**, 5887 (2012).

[45] I. Martin, What is the expected return on the market? Q. J. Econ. **132**, 367 (2017).

[46] E. Torrontegui, S. Ibánez, S. Martínez-Garaot, M. Modugno, A. del Campo, D. Guéry-Odelin, A. Ruschhaupt, X. Chen, and J. G. Muga, Chapter 2 - Shortcuts to adiabaticity, Adv. At. Mol. Opt. Phys. **62**, 117 (2013).

[47] D. Guéry-Odelin, A. Ruschhaupt, A. Kiely, E. Torrontegui, S. Martínez-Garaot, and J. G. Muga, Shortcuts to adiabaticity: Concepts, methods, and applications, Rev. Mod. Phys. **91**, 045001 (2019).

[48] D. Sels and A. Polkovnikov, Minimizing irreversible losses in quantum systems by local counterdiabatic driving, Proc. Natl. Acad. Sci. USA **114**, E3909 (2017).

[49] A. Hartmann, V. Mukherjee, G. B. Mbeng, W. Niedenzu, and W. Lechner, Multi-spin counter-diabatic driving in many-body quantum Otto refrigerators, Quantum **4**, 377 (2020).

[50] S. Iram, E. Dolson, J. Chiel, J. Pelesko, N. Krishnan, Ö. Güngör, B. Kuznets-Speck, S. Deffner, E. Ilker, and J. G. Scott,

Controlling the speed and trajectory of evolution with counter-diabatic driving, Nat. Phys. **17**, 135 (2021).

[51] P. W. Claeys, M. Pandey, D. Sels, and A. Polkovnikov, Floquet-Engineering Counterdiabatic Protocols in Quantum Many-Body Systems, Phys. Rev. Lett. **123**, 090602 (2019).

[52] N. N. Hegade, X. Chen, and E. Solano, Digitized-counterdiabatic quantum optimization, Phys. Rev. Res. **4**, L042030 (2022).

[53] Quantinuum H1-1 emulator, https://www.quantinuum.com, September 10-12, 2022.

[54] L. Zhu, H. L. Tang, G. S. Barron, F. A. Calderon-Vargas, N. J. Mayhall, E. Barnes, and S. E. Economou, Adaptive quantum approximate optimization algorithm for solving combinatorial problems on a quantum computer, Phys. Rev. Res. **4**, 033029 (2022).

[55] S. Hadfield, Z. Wang, B. O'Gorman, E. Rieffel, D. Venturelli, and R. Biswas, From the quantum approximate optimization algorithm to a quantum alternating operator ansatz, Algorithms **12**, 34 (2019).

[56] D. Headley, T. Müler, A. Martin, E. Solano, M. Sanz, and F. K. Wilhelm, Approximating the quantum approximate optimization algorithm with digital-analog interactions, Phys. Rev. A **106**, 042446 (2022).

[57] S. Ruder, An overview of gradient descent optimization algorithms, arXiv:1609.04747.